Advanced Synthesis & Catalysis

Accepted Article

Title: Loop Swapping as a Potent Approach to Increase Ene Reductase Activity with Nicotinamide Adenine Dinucleotide (NADH)

Authors: Christoph Mähler, Franziska Kratzl, Melina Vogel, Stefan Vinnenberg, Dirk Weuster-Botz, and Kathrin Castiglione

To be cited as: *Adv. Synth. Catal.* 10.1002/adsc.201900073

Link to VoR: http://dx.doi.org/10.1002/adsc.201900073

 10.1002/adsc.201900073

Loop Swapping as a Potent Approach to Increase Ene Reductase Activity with Nicotinamide Adenine Dinucleotide (NADH)

Christoph Mähler,[a] Franziska Kratzl,[a] Melina Vogel,[a] Stefan Vinnenberg,[a] Dirk Weuster-Botz,[a] and Kathrin Castiglione[b,*]

[a] Technical University of Munich, Institute of Biochemical Engineering, Boltzmannstr. 15, D-85748 Garching, Germany

[b] Friedrich-Alexander-University Erlangen-Nürnberg, Institute of Bioprocess Engineering, Paul-Gordan-Str. 3, D-91052 Erlangen, Germany

Key words: Alkene reduction, Biocatalysis, Cofactors, Ene reductase, Loop swapping, Protein engineering

* Corresponding author:
Telephone: +49 9131 85 23003
Fax: +49 9131 85 23002
Email: kathrin.castiglione@fau.de
Homepage: https://www.bvt.tf.fau.de

10.1002/adsc.201900073

Abstract

The asymmetric reduction of alkenes is a widely used transformation in industry. Ene reductases (ERs) are $(\beta\alpha)_8$-barrel folded enzymes capable of catalyzing this hydrogenation reaction. At the expense of nicotinamide coenzymes, ERs can reduce a wide range of electron-deficient alkenes in an anti-specific manner and with high regio- and stereoselectivities. However, a cost-effective industrial use of these enzymes is hampered, since most ERs prefer nicotinamide adenine dinucleotide phosphate (NADPH) to the more stable and less expensive non-phosphorylated nicotinamide adenine dinucleotide (NADH) as coenzyme. Here, we demonstrate an approach to both modify the biocatalysts coenzyme selectivity and strongly increase the activity and affinity with NADH. By swapping loop regions of the cyanobacterial NostocER1 for the corresponding regions of two NADH-favoring ERs, a strong alteration of the biocatalyst's coenzyme binding was achieved. This made possible a transfer of the respective donor-ER kinetic parameters to NostocER1. Additionally, outperformance of both donors in terms of activity was achieved through combinatorial swapping of loops of both species. These findings demonstrate the high potential of loop swapping as protein engineering approach to selectively optimize the coenzyme binding of ERs.

10.1002/adsc.201900073

Introduction

The industrial demand for enantiopure products is steadily increasing.[1] The asymmetric hydrogenation of alkenes represents one way to synthesize pure enantiomers or diastereomers. Whereas *syn*-hydrogenations are mostly accomplished with expensive chiral metal complexes,[2] *anti*-hydrogenations can be achieved using biocatalysts, i.e. ene reductases (ERs). ERs are of potential interest for industrial processes not only due to their high regio-, stereo- and enantioselectivity, but also because of a broad substrate spectrum.[3,4] The substrates are alkenes bearing an electron-withdrawing group (EWG) such as α, β-unsaturated ketones, aldehydes, carboxylic acids, esters, imides, nitriles, and nitroalkenes.[4] In this context the most investigated class of ERs are flavin-dependent oxidoreductases of the old yellow enzyme family (OYEs, EC 1.6.99.1). The reduction proceeds via a ping-pong bi-bi mechanism, thus the catalytic cycle of ERs is separated in two half reactions: a reductive and an oxidative half reaction (Scheme 1).[5,6] The reductive half reaction comprises a hydride transfer from NAD(P)H to the enzyme-bound prosthetic group, flavin mononucleotide (FMN), and the release of oxidized $NAD(P)^+$.[7] During the oxidative half reaction this hydride reduces the electron deficient double bond in an anti-specific manner creating up to two stereogenic centers.[6] All currently known members of the OYE family have essentially the same tertiary structure, an $(\beta\alpha)_8$-barrel structure or so-called triose phosphate isomerase (TIM)-barrel fold.[4] This means that, eight alternating α-helices and parallel β-sheets form a barrel-like structure, in which the sheets shape the inner wall and the helices the outer wall of the barrel. The enzymes' active site, comprising the FMN-binding site, is located on top of this barrel, formed by the flexible loop regions between the C-terminal ends of the β-sheets and the N-terminal ends of the α-helices.[4,8] These loops, as well as the corresponding secondary structure elements, are numbered consecutively beginning with 1 at the N-terminus and ending with 8 at the C-terminus.

Although many wild type ERs possess desirable properties like a broad substrate spectrum and high stereoselectivities, protein engineering has been successfully applied to change unwanted characteristics of these biocatalysts.[9] For instance, a small active site limiting the

10.1002/adsc.201900073

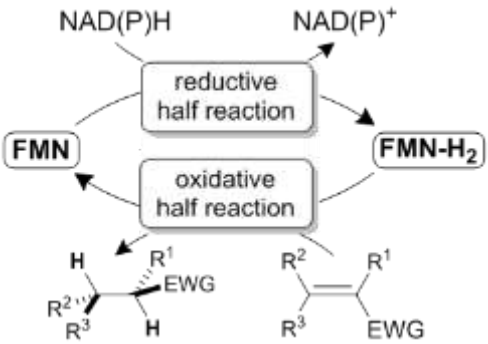

Scheme 1. The catalytic cycle of OYEs is separated in two half reactions. The reductive half reaction comprises a hydrid transfer from NAD(P)H to the enzyme-bound FMN, generating a reduced FMN-H_2. During the oxidative half reaction FMN-H_2 reduces the alkene bearing an electron-withdrawing group (EWG), transferring the OYE back to the starting point carrying an oxidized FMN.

substrate size was altered through changes of the active site entrance,[10] or rational mutagenesis was applied to alter the enzymes stereoselectivity.[11] Another example is the modulation of the substrate scope through exchanges of loop regions.[12] However, the industrial use of ERs remains hampered since the majority of OYEs prefer NADPH to the less expensive and more stable NADH as coenzyme.[4,8,13] Additionally, the variety of NADH-regenerating enzymes is higher than for its phosphorylated derivative,[14] facilitating the application of NADH-preferring biocatalysts in industrial bioprocesses.[15] Since an undesired coenzyme selectivity is a common phenomenon among oxidoreductases, coenzyme engineering has emerged as an important area of protein engineering.[14,16] All approaches to alter enzymatic coenzyme binding can be categorized into three major groups: random, rational and semi-rational.[14] The application of knowledge-free random approaches like error-prone PCR or gene shuffling are rarely used for changing coenzyme binding since beneficial changes are nearly always limited to the coenzyme binding site[17] and screening of large libraries is labor, time and material intensive.[14] Rational approaches mostly focus on the change of specific residues responsible for coenzyme binding.[18] This requires a deep understanding of coenzyme binding, which is in most cases neither easily determinable nor transferable through structural diversity within an enzyme family, let alone a common protein fold.[19] Driven by computational tools and algorithms, semi-rational approaches have become increasingly relevant for coenzyme engineering.[14,16] Through different techniques,

10.1002/adsc.201900073

potential hot spots for coenzyme engineering can be identified and used to create 'small but smart' libraries.[20] In this context, a promising, easy-to-use web tool called Cofactor Specificity Reversal-Structural Analysis and Library Design (CSR-SALAD) was established and successfully applied.[17,21] CSR-SALAD detects and classifies residues that determine cofactor specificity and designs degenerated codon libraries. However, a reliable and detailed knowledge about the interactions of coenzyme and protein is inevitable for the application of these computational tools. Furthermore, natural evolution phenomena like insertions or deletions are not considered.[16]

Another semi-rational approach to influence coenzyme binding that requires less pre-knowledge and includes natural evolution is the modulation of whole protein parts. This can span from swapping of short loops[22] up to entire binding pockets.[14] In this context, probably the best-known example is the adjustment of the nucleoside ribose 2' binding-site of dehydrogenases possessing a Rossmann-fold. Thus, by exchanging two loops it was possible to transfer the preference for NADP(H) from an α-keto acid reductase from *Sphingomonas* sp. A1 named A1-R to the homologue A1-R'.[23] Similar results could be achieved through exchange of one loop of a malate dehydrogenase[24] and an isopropylmalate dehydrogenase.[25] Loop swapping was also applied to engineer a NADP-dependent Rossmann-folded isocitrate dehydrogenase to NAD-dependency.[26] However, the exchange of entire loops to influence coenzyme binding in other protein folds, particularly in the widespread $(\beta\alpha)_8$-barrel fold, was rarely applied so far.[16] This is surprising since loop swapping among enzymes possessing this fold is seen highly promising.[27] Additionally, it was successfully applied to transfer substrate specifities,[12,28,29] whereby partly an unexpected modification of coenzyme binding occurred.[12,29] For these reasons, we demonstrate in this work the high potential of loop swapping as engineering strategy to selectively control coenzyme binding of $(\beta\alpha)_8$-barrel folded ERs.

10.1002/adsc.201900073

Results and Discussion

The aim of the work was to influence the coenzyme preference as well as to increase the activity and affinity of an OYE towards NADH. This should be accomplished with a low screening effort. The cyanobacterial ene reductase 1 from *Nostoc* sp. PCC7120 (NostocER1) was used as scaffold. This 'acceptor' enzyme is characterized by a very high stereoselectivity with a broad substrate spectrum. Furthermore, NostocER1 exhibits high activity with its natural coenzyme NADPH, revealing the enzyme's fast oxidative half reaction.[30] However, like most OYEs, NostocER1 has a strong preference towards NADPH, as indicated by a more than 20-fold higher catalytic efficiency (k_{eff}) compared to NADH.

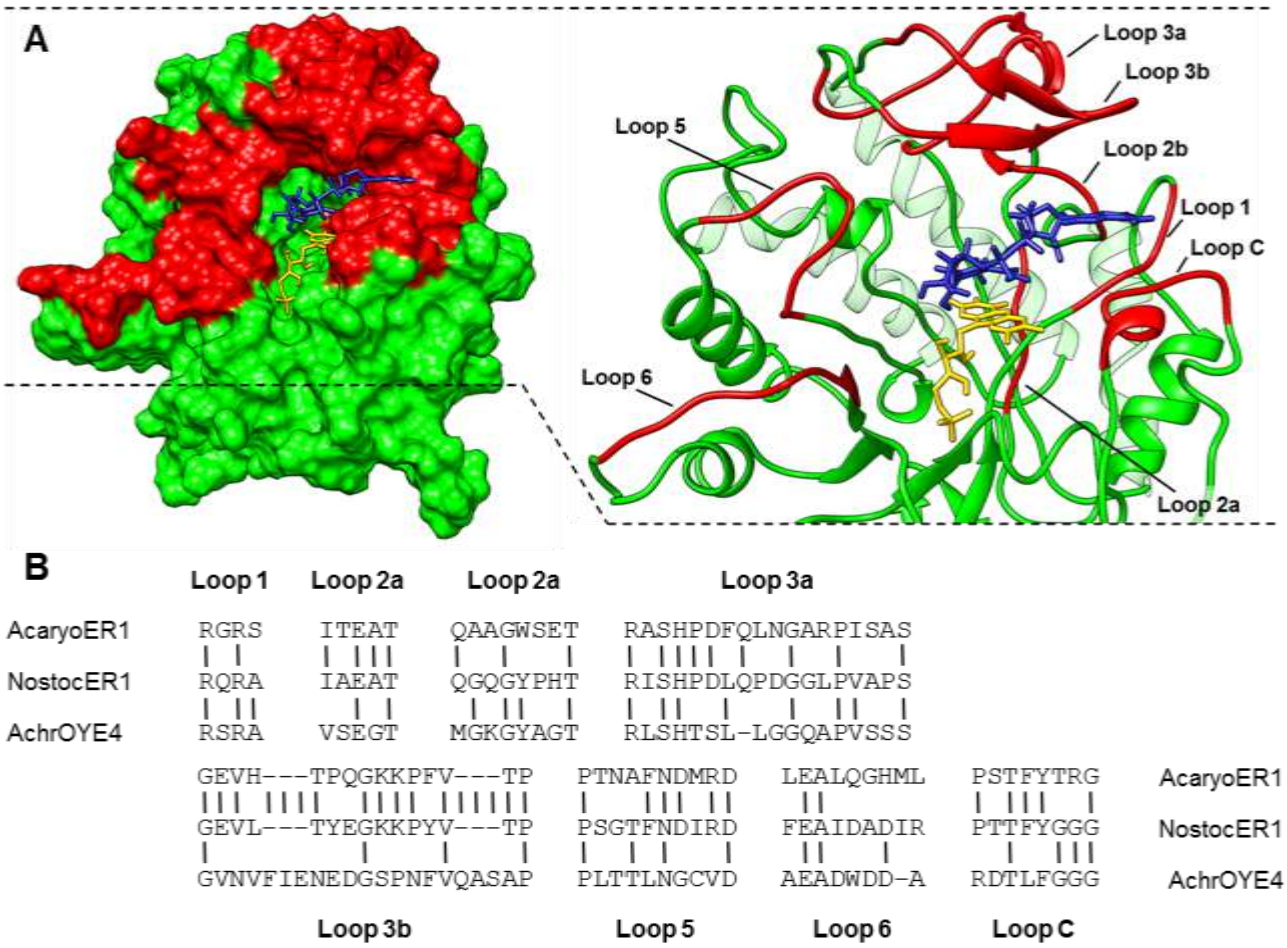

Figure 1. **A** Homology model of NostocER1 (green) based on morphinone reductase crystal structure (PDB: 2r14). The coenzymes FMN (yellow) and NADH (blue) are depicted bound in the active site, as well as all loop regions (red) that have been exchanged. **B** Sequence alignment of the exchanged loop regions.

10.1002/adsc.201900073

Swapping of single loop regions

In order to alter the biocatalyst's dependency on the phosphorylated coenzyme, we identified and systematically exchanged all loop regions that might have a direct interaction with the coenzyme (Figure 1A). Due to their size, Loop 2 and 3 have been divided into two possible contact areas (a and b), and the contact area after Loop 8 between Helix 8 and the C–terminus is labeled Loop C. Loops 7 and 8, as well as Loop 4, have not been exchanged because of their presumed long distance to the coenzyme binding site or high primary structure identity, respectively. The eight dedicated protein regions have been exchanged for the corresponding regions originating from two different 'donor' enzymes. On the one hand, the cyanobacterial ene reductase 1 from *Acaryochloris marina* (AcaryoER1) was used due to its high activity with NADH.[30] On the other hand, the more distantly related proteobacterial Old Yellow Enzyme 4 from *Achromobacter* sp. JA81 (AchrOYE4) was employed because of its high affinity towards NADH.[31] This resulted in various modifications of the loops, ranging from single point mutations to the exchange of up to 17 amino acids, including insertions and deletions (Figure 1B). Thereby, our goal was to swap these NADH-binding properties without transferring undesired donor properties, e.g. a slow substrate reduction during the oxidative half reaction.

Figure 2 shows the specific activities using 200 µM NADH (v_{200}) and 10 mM maleimide as substrate of the eight NostocER1-AcaryoER1 hybrid enzymes (blue columns) and the eight NostocER1-AchrOYE4 hybrid enzymes (red columns) in comparison to the wild type enzymes (WTs). The activities with 200 µM NADH were chosen for an initial comparison, since most industrial biotransformations are operated with catalytical amounts of coenzyme in order to reduce costs.[32] Already five out of sixteen of these single loop exchanges showed the intended increased activity compared to NostocER1. The exchange of Loop 2a and 3b with the corresponding regions of AcaryoER1 led to a 2.2- or 1.5-fold increased activity. The exchange of the NostocER1 Loop 1 with the complementary region of AchrOYE4 resulted in a remarkable 6.6-fold increased activity of 14.5 ± 1.5 U mg^{-1}. This hybrid enzyme was the only one of these single loop swaps outperforming its 'donor' enzyme

10.1002/adsc.201900073

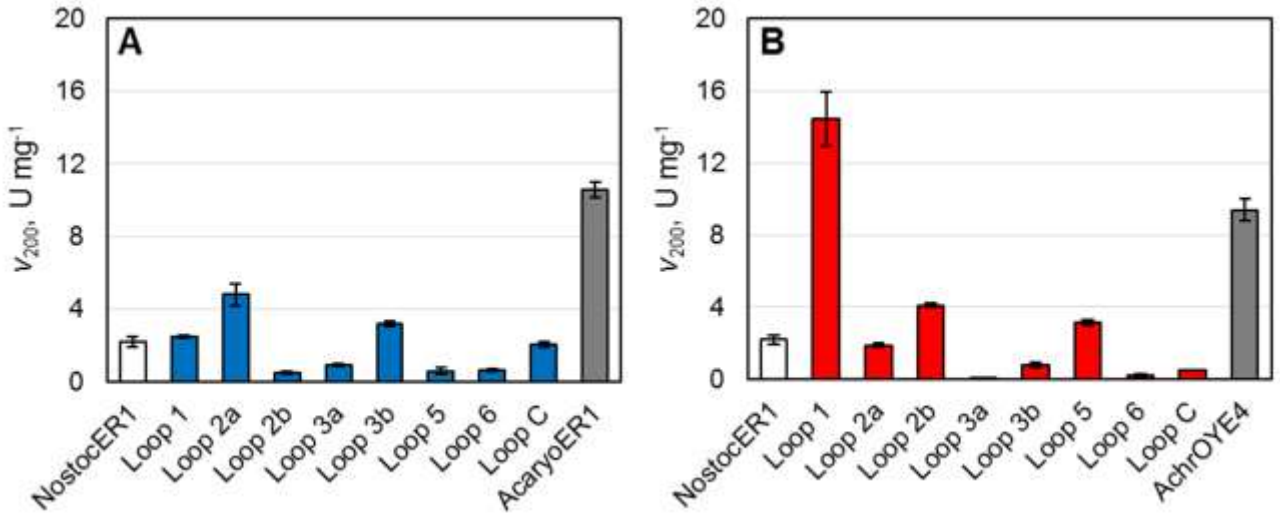

Figure 2. Specific activities using 200 µM NADH (v_{200}) of the 'acceptor' enzyme NostocER1 (white), the 'donor' enzymes AcaryoER1 and AchrOYE4 (gray) and the corresponding hybrid enzymes of NostocER1 and AcaryoER1 loop regions (blue, **A**) or NostocER1 and AchrOYE4 (red, **B**). The values are means of at least two biological replicates (m) with five technical replicates each. Divergent biological replications were applied for NostocER1 (m = 6), the NostocER1-AcaryoER1 Loop swaps 1 (m = 3), 2a (m = 4), 5 and 8 (m = 3), AcaryoER1 (m = 4), the AchrOYE4 Loop swap 1 (m = 5), and AchrOYE4 (m = 5).

AchrOYE4 in terms of activity under these conditions. Furthermore, the alteration of Loop 2b enhanced the v_{200} 1.9-fold, the one of Loop 5 1.4-fold.

Interestingly, the insertion of AcaryoER1 and AchrOYE4 loops didn't reveal a common NostocER1 'target loop' to augment its NADH activity. Four of the five identified loop changes that increase the activity of NostocER1, i.e. Loop 1, 2a, 2b, 3b, are positioned close to the adenine-moiety of the coenzyme. This is hardly surprising, since the phosphate group (which is the only feature that distinguishes NADPH from NADH) is located close to these loops, making them to a common target for coenzyme engineering.[17,21] Moreover, a larger number of loops close to this area has been swapped, thus increasing the probability of a positive change. Nonetheless, the exchange of Loop 5 represents one target area close to the nicotinamide moiety which is spatially more distant to the adenine moiety. By applying a more rational method, this target area likely could have been lost.

In addition, the v_{200} values with NADPH were determined (Supporting Information, Figure S2). All hybrids with an increased NADH activity showed either no significant change or only a slightly decreased NADPH activity compared to NostocER1, with the exception of

10.1002/adsc.201900073

Table 1. Kinetic parameters catalytic constant (k_{cat}), Michaelis-Menten constant (K_m) and the catalytic efficiency (k_{eff}) of the wild type enzymes and hybrid enzymes showing an increased specific activity with NADH. Additionally shown is the relative catalytic efficiency (RCE), which describes the ratio of the enzyme's k_{eff} with NADH and NostocER1's k_{eff} with NADPH. The kinetic parameters are the result of at least one nonlinear regression. Divergent biological replication was applied for the WTs NostocER1 (m = 3), AcaryoER1 (m = 2), AchrOYE4 (m = 2), the ArchOYE4 Loop 1 exchange (m = 2) and the Loop 1,5 exchange (m = 2). The depicted means and standard deviations were calculated according to equation 1 and 3.

Enzyme	Donor	k_{cat}, s^{-1}	K_m, µM	k_{eff}, s^{-1} mM^{-1}	RCE[c], -
NostocER1[a]	-	15.2 ± 1.9	1050 ± 220	14.4 ± 3.5	0.04
AcaryoER1[a]	-	19.8 ± 2.3	351 ± 46	56.2 ± 9.8	0.17
AchrOYE4[a]	-	9.0 ± 0.2	57 ± 17	157 ± 47	0.47
Loop 2a[a]	AcaryoER1	20.3 ± 1.3	805 ± 91	25.3 ± 3.3	0.08
Loop 3b[a]	AcaryoER1	13.4 ± 0.4	768 ± 48	17.5 ± 1.2	0.05
Loop 1[a]	AchrOYE4	18.2 ± 0.2	190 ± 14	95.5 ± 7.3	0.29
Loop 2b[a]	AchrOYE4	10.3 ± 0.3	535 ± 33	19.2 ± 1.3	0.06
Loop 5[a]	AchrOYE4	8.9 ± 0.2	633 ± 34	14.0 ± 0.8	0.04
Loop 2a,3b[a]	AcaryoER1	19.2 ± 0.4	237 ± 17	81.1 ± 6.2	0.24
Loop 1,2b[a]	AchrOYE4	16.5 ± 0.4	474 ± 31	34.7 ± 2.4	0.10
Loop 1,5[a]	AchrOYE4	8.6 ± 0.9	73 ± 13	119 ± 25	0.36
Loop 1,2a[a]	both donors	29.1 ± 0.4	224 ± 11	130 ± 6.7	0.39
Loop 1,3b[a]	both donors	15.1 ± 0.5	430 ± 37	35.2 ± 3.2	0.11
Loop 1,2a,3b[a]	both donors	21.7 ± 0.6	413 ± 29	52.6 ± 4.0	0.16
Loop 1,5,2a[a]	both donors	19.0 ± 0.4	161 ± 11	118 ± 8.7	0.36
Loop 1,5,2a,3b[a]	both donors	15.0 ± 0.3	241 ± 18	62.3 ± 4.8	0.19
NostocER1[b]	-	26.7 ± 0.9	80 ± 19	333 ± 78	1.00

[a] Kinetic parameters for NADH
[b] Kinetic parameters for NADPH
[c] Relative catalytic efficiency (RCE)

the already mentioned Loop 5 swap. This hybrid has a strongly decreased NADPH activity, represented by a 13.6-fold lower v_{200} compared to NostocER1. Thus, the loop seems to be associated with the low NADPH-activity of AchrOYE4 (v_{200} of 0.07 ± 0.01 U mg^{-1}) and the enzymes distinct coenzyme specificity.

The improved enzyme variants were characterized in detail. The catalytic constants (k_{cat}) and Michaelis-Menten constants (K_m) of the five identified hybrids with an increased NADH activity and of the three wild type enzymes are listed in Table 1. A graphical comparison of these values is shown in the Supporting Information, Figure S3. In Figure S4, exemplary plots of the data used for the parameter estimation by non-linear regression analysis are

10.1002/adsc.201900073

shown. It can be seen that the two NostocER1-AcaryoER1 hybrid enzymes only have a slightly higher affinity towards NADH than NostocER1, with K_m values around 800 µM. A comparable picture emerges from the NostocER1-AchrOYE4 hybridizations Loop 2b and 5, showing a reduced K_m of around 600 µM. The Loop 1 alteration once again reveals the biggest improvement, reducing the K_m by a factor of more than 5 from 1050 ± 220 µM to 190 ± 14 µM. However, none of the single swaps could transfer the corresponding wildtype K_m to NostocER1.

To exclude negative influences caused by the loop swaps, expression levels and thermal stabilities of the hybrids were checked. All hybrids with an increased NADH activity could be isolated in quantities ranging from 21.3 to 67.4 mg $L_{culture}^{-1}$. These values are comparable to the results obtained for the wildtype since nine independent expressions and purifications of NostocER1 resulted in an average isolated protein amount of 40.8 ± 11.2 mg per liter culture. Additionally, the hybrids with the exchanged Loops 1, 2b and 5 were randomly chosen for a comparative analysis of the thermal stability at 40 °C. These experiments revealed no decrease in thermal stability compared to the NostocER1 wildtype.

Swapping of multiple loop regions

Combinations of the five identified loops were applied in order to evaluate whether a further increase in activity with or affinity for NADH is accessible. Therefore, separate combinations of both ‘donor’ enzymes were conducted initially, leading to one NostocER1-AcaryoER1 and four NostocER1-AchrOYE4 hybridizations. As a first comparison, the v_{200} values of these mutants were compared to the values of the wildtypes (Supporting Information, Figure S5A). Three out of five multiple loop swapped enzymes showed a specific activity comparable to the one of the ‘donors’. In particular, the combination of the two AcaryoER1 Loops 2a and 3b led to a further positive effect, resulting in a 5.5-fold higher specific activity of 11.9 ± 0.7 U mg^{-1}. This is also reflected by its kinetic parameters. The hybrid has a similar k_{cat} (19.2 ± 0.4 s^{-1}) and a slightly decreased K_m (237 ± 17 µM) compared to the ‘donor’ AcaryoER1 (Table 1). Although the four combinations of the exchanged AchrOYE4 Loops 1,

10.1002/adsc.201900073

2b and 5 resulted in no further increase of activity, a remarkable result could be achieved in terms of the K_m (Table 1 and Supporting Figure S6). The K_m of the NostocER1-AchrOYE4 Loop 1,5 hybridization was further decreased to 73 ± 13 µM, which means that no significant difference between the K_m of the hybrid enzyme and the excellent K_m of its 'donor' AchrOYE4 is observable. Consequently, the swapping of two loops of each of the 'donors' enabled the transfer of both kinetic parameters k_{cat} and K_m to the 'acceptor' enzyme NostocER1.

Furthermore, we combined the most promising loops, i.e. AcaryoER1 Loop 2a and 3b as well as AchrOYE4 Loop 1 and 5, to determine whether outperforming of both donors in terms of activity and affinity is possible. Thus, five additional multiple loop swaps were generated. Remarkably, all combinations with this set of loops showed at least a similar k_{cat} and a by a factor of 2.5 reduced K_m compared to NostocER1, indicating the excellent combinability of the determined protein loops (Table 1 and Supporting Figure S7). One loop combination with a strongly increased activity could be identified, namely AcaryoER1 Loop 2a merged with AchrOYE4 Loop 1. The Loop 1,2a-hybrid even resulted in the highest detected activity with a k_{cat} of 29.1 ± 0.4 s^{-1}, which corresponds to a 1.9-fold increased value compared to the 'acceptor' enzyme NostocER1. The Michaelis-Menten constants of these hybrid enzymes containing loops of both donors were between 161 µM and 430 µM, which means that no further improved K_m could be detected.

The v_{200} values with NADPH of all multiple loop swaps are shown in Supporting Information, Figure S8. A result comparable to the single loop swaps was obtained. The hybrids v_{200} values were in the region of the v_{200} of NostocER1, ranging between a maximal increase of 50 % and decrease of 30 % in comparison to the wildtype. The sole exceptions are again the hybrids comprising the Loop 5 originating from AchrOYE4. These mutants showed a drastically reduced activity of up to 90 %. This is a further indication for the low NADPH acceptance associated with this loop. Thus, besides increasing the affinity towards NADH, AchrOYE4 Loop 5 can additionally be used to strongly increase the selectivity towards

10.1002/adsc.201900073

NADH. Depending on the application, it can be desirable that the biocatalyst uses only one coenzyme.[16]

Valuation of NostocER1 engineering

As additional comparison between the 'best performers' and the wild type enzymes, the catalytic efficiency (k_{eff}) for NADH was calculated (Table 1). The k_{eff} of the best single swap (AchrOYE4 Loop 1) was already more than 6-fold higher than the one of NostocER1. The efficiencies of the best multiple loop swaps, i.e. the various combinations of AchrOYE4 Loop 1, Loop 5 and AcaryoER1 Loop 2a, were 8- to 9-fold higher. Six hybrid enzymes could be created that had a higher k_{eff} than the cyanobacterial 'donor' AcaryoER1 and three of the multiple loop exchanges showed no significant difference to the proteobacterial 'donor' AchrOYE4. To assess the engineering success, the kinetic parameters of NostocER1 using its preferred coenzyme NADPH are additionally listed. With a k_{cat} of 29.1 ± 0.4 s^{-1}, the Loop 1,2a hybrid outperformed the wildtype's NADPH catalytic constant (26.7 ± 0.9 s^{-1}) and the Loop 1,5 hybrid yielded in a similar K_m (73 ± 13 µM) compared to the one of NostocER1 with NADPH (80 ± 19 µM). As a further comparison, the relative catalytic efficiency (RCE), i.e. the ratio of the enzyme's k_{eff} with NADH and the NostocER1 WT with NADPH, was used. Three multiple loop swaps with the highest determined k_{eff} values between 118 ± 8.7 s^{-1} μM^{-1} and 130 ± 6.7 s^{-1} μM^{-1} yielded an RCE from 0.36 to 0.39. Up to now, there have been 51 oxidoreductase mutants with an altered coenzyme specificity towards NAD(H) described in the literature. Only 11 of them possess a higher RCE.[16] Furthermore, 9 out of these 11 engineered enzymes have a Rossmann-like cosubstrate binding domain, for which cosubstrate engineering is already well-understood. On the contrary, successful changes of coenzyme specificity of enzymes belonging to EC 1.6 are very rare and coenzyme engineering of oxidoreductases possessing a prosthetic group, e.g. a flavo-group, tend to be more challenging.[16] These facts underpin the high potential of the presented optimization approach.

10.1002/adsc.201900073

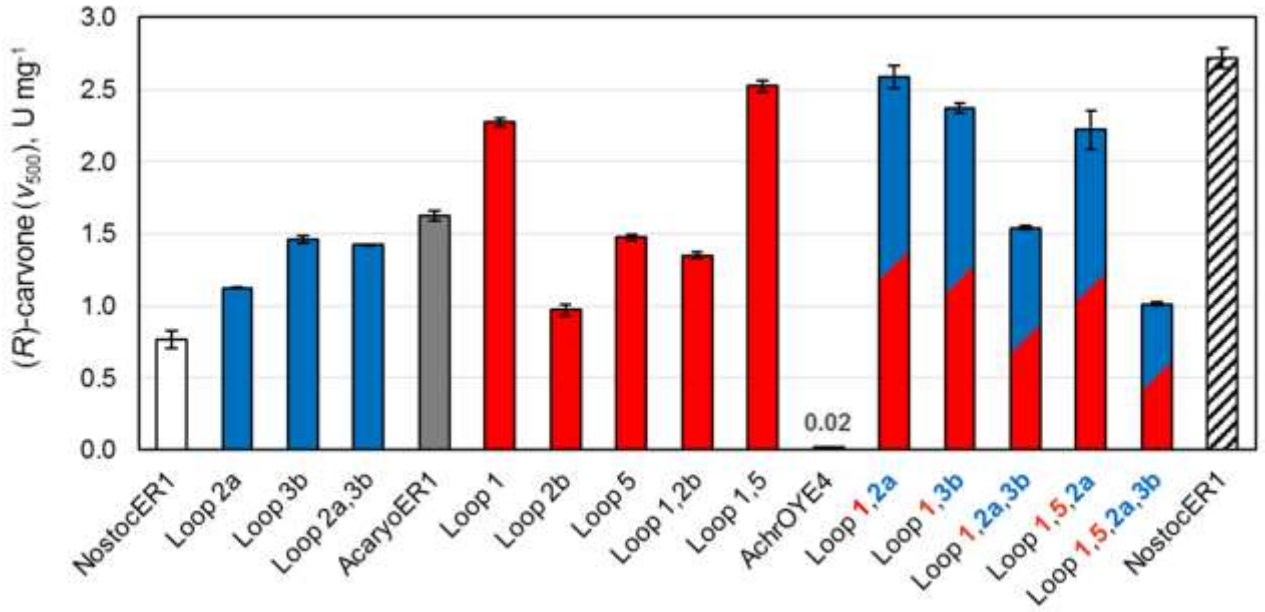

Figure 3. Specific activities with 500 µM NADH (v_{500}) and 10 mM (*R*)-Carvone of the NostocER1 (white), the 'donor' enzymes AcaryoER1 and AchrOYE4 (gray), the hybrid enzymes of NostocER1 with AcaryoER1 loop regions (blue), NostocER1 with AchrOYE4 loop regions (red) and NostocER1 with loop regions of both 'donors' (blue/red). Depicted in addition is the specific activity of NostocER1 with 500 µM NADPH and 10 mM (*R*)-carvone (white/black). The v_{500} values are means of three technical replicates. Additional biological replication was applied for NostocER1 (m = 3 (NADH) / m = 2 (NADPH)), AcaryoER1 (m = 2), and the Loop combination 1,2a (m = 3).

Enhanced dihydrocarvone synthesis

Finally, we evaluated the specific activities of the reduction of the substrate (*R*)-carvone to (2*R*,5*R*)-dihydrocarvone (Supporting Information, Figure S9A). Dihydrocarvone has industrial relevance due to its use in the synthesis of natural products, e.g. tetraoxane derivatives as compounds with antimalarial activity,[33] or keto decalin derivatives as insect antifeedants.[34] Due to the higher detection limits of the gaschromatographic analysis, an assay with a higher NADH concentration (500 µM, v_{500}) was applied. Like a variety of organic substrates,[35] the water solubility of (*R*)-carvone is low.[36] Thus, the applied substrate concentration (10 mM) was close to the applicable maximum. Furthermore, in order to reduce toxicity on the biocatalyst and to overcome these low substrate solubilities, biocatalytic transformations on a laboratory or industrial scale are often conducted in aqueous biphasic systems.[37] Therefore, only catalytic activities using low substrate concentrations are of interest. The specific activities for the WT enzymes and all hybrids with an increased NADH activity are shown in

10.1002/adsc.201900073

Figure 3. All identified hybrid enzymes possessing an increased activity with the coenzyme showed a faster conversion of (*R*)-carvone using NADH. Similar to the previous results, the biggest increase of activity was achieved by the enzymes possessing the highest k_{eff} values with NADH, i.e. the swapping of AchrOYE4 Loop 1, and additional combinations with AchrOYE4 Loop 5 and/or AcaryoER1 Loop 2a. Interestingly, one additional hybrid with a lower k_{eff} possessed an activity comparable to these 'best performers', the combination of AcaryoER1 Loop 3b with AchrOYE4 Loop 1. These five enzymes had an activity between 2.27 ± 0.03 U mg^{-1} (Loop 1 swap) and 2.59 ± 0.08 U mg^{-1} (Loop 1,2a swap), which represented an up to 3.4-fold increased activity compared to NostocER1 (0.77 ± 0.06 U mg^{-1}). Special emphasis is placed on comparing the activity of these five hybrid enzymes and the NostocER1 activity using 500 µM NADPH. The hybrids only possess a marginal lower or not significantly different specific activity, revealing a shift of the rate-limiting step from the reductive half reaction to the oxidative half reaction. The fact that the extremely low activity of AchrOYE4 with (*R*)-carvone (0.02 ± 0.01 U mg^{-1}) was not transferred to any of the hybrid enzymes comprising AchrOYE4 loops deserves additional highlighting. Furthermore, no negative influence on NostocER1's excellent stereoselectivity could be observed. None of the hybrids showed a significant increase in (2*S*,5*R*)-dihydrocarvone byproduct formation, represented by a preservation of the wildtypes desirable diastereomeric ratio of 99.4 ± 0.5 % (Supporting Information, Figure S9B). The fact that none of the hybrids revealed a change in (*R*)-carvone binding points towards a preservation of NostocER1's excellent substrate spectrum and stereoselectivity. However, since the main focus of this work was on engineering the reductive half-reaction, a detailed characterization of the oxidative half reaction of the loop swapped hybrids remains part of further studies.

Conclusions

We could demonstrate that the systematic exchange of loop regions involved in coenzyme binding is a potent approach to alter coenzyme binding. Thus, we could strongly increase the activity and affinity with NADH of a cyanobacterial ER. By using a homology model, we

10.1002/adsc.201900073

determined eight target loop regions of NostocER1 that might interact with the coenzyme and swapped these with the corresponding regions of two donor ERs possessing a high activity with NADH (AcaryoER1) or a high affinity (AchrOYE4) towards NADH. We could identify five engineered ERs showing the desired higher activity with and affinity towards the coenzyme through the generation of only 16 loop swapped proteins. These five hybrids included one 'unexpected' target area more distant to the adenine moiety of NAD(P)H, where an enzyme's specificity to one of the coenzymes typically originates from. This hit likely could have been missed by applying a more rational engineering approach. Combination of the five identified target loops enabled not only the transfer of the donor enzymes reductive half reaction characteristics to NostocER1, but also the outperformance of both donors in terms of activity. Additionally, some hybrids showed increased or unchanged activity with NADPH, some showed a strongly decreased NADPH activity. Depending on the application, it can be desirable that the biocatalysts use selectively only one or both coenzymes.[16] Moreover, no undesired characteristics were transferred through this engineering approach. The NostocER1 hybrids showed no changes in the wildtypes' excellent stereoselectivity. These findings demonstrate the high potential of loop swapping as enzyme engineering technique with a low screening effort to selectively influence coenzyme binding in a $(\beta\alpha)_8$-folded ERs.

Experimental Section

Recombinant enzyme expression and purification

Chemically competent *E. coli* BL21 (DE3) cells (Novagen, San Diego, CA) were transformed for protein expression and cultivated on Lysogeny broth (LB) agar plates supplemented with 35 mg L^{-1} kanamycin. Preculture preparation was performed in 4 mL Terrific Broth supplemented with 35 mg L^{-1} kanamycin (TB-Kan), inoculated with a single colony and incubated overnight (13 mL polypropylene tubes, 30°C, 250 rpm, 5 cm excentricity). 1 L shaking flasks without baffles supplemented with 200 mL TB-Kan were inoculated with 1 mL preculture and cultivated (37°C, 200 rpm, 5 cm excentricity) until an attenuance at 600 nm (OD_{600}) of 0.6 was reached. Cultivation media was cooled to 20 °C on ice and expression

10.1002/adsc.201900073

was induced using by adding 200 µM isopropyl β-D-thiogalactoside (IPTG). Thereafter, cells were cultivated (20 °C, 250 rpm, 3.5 cm excentricity) for exactly 20 h and collected by centrifugation (3260 g, 4°C, 5 min).

The harvested cells containing ERs with an *N*-terminal His_6-tag were purified via affinity chromatography using HisPur™ Ni-NTA Spin Columns (Thermo Fisher Scientific, Waltham, MA). After cell lysis in 5-times the cell wet weight EQ-buffer (20 mM sodium phosphate, 300 mM sodium chloride with 20 mM imidazole, pH 7.4) via sonication, purification was performed at 4°C according to the manufacturer's protocol, with the exception that an imidazole concentration of 55 mM in the wash buffer was applied. Buffer exchange to 100 mM sodium phosphate buffer, using a minimal protein solution to buffer ratio of 1:200, was applied via dialysis (4°C, overnight) using ZelluTrans membranes (Carl Roth, Karlsruhe, Germany; cutoff 14 kDa).

Protein analysis

Protein concentration was determined using the Pierce™ BCA Protein Assay Kit (Thermo Fisher Scientific, Waltham, MA). Enzymatic purity and size were determined via SDS-PAGE using 3% and 12.5% Bis-Tris gels in Tris-glycine running buffer with JustBlue Prestained Protein Marker (NIPPON Genetics EUROPE, Düren, Germany). Gels were stained according to Fairbanks and coworkers.[38]

Enzyme assay

Enzyme activity was determined by a photometric assay measuring the decrease of NAD(P)H at 340 nm using a molar absorption coefficient of 6.22 mM^{-1} cm^{-1}. Reactions were performed using 1.5 - 500 µg mL^{-1} purified enzyme in sodium phosphate buffer (100 mM, pH 7.0). Assays were conducted at 30 °C using F96 microwell plates (Nunc, Roskilde, Denmark) and a Multiscan™ FC Photometer (Thermo Fisher Scientific, Waltham, MA). Measurements were recorded for 10 min and 100 data points. Reactions were initiated by the addition of 10 mM maleimide as substrate. Reaction rates were determined by

10.1002/adsc.201900073

automated linear regression using MATLAB R2015b (The MathWorks, Natick, MA). The maximal rate of decrease was calculated for at least 2 min (20 data points) and a minimal R^2 of 0.995. One unit of enzyme activity (U) was defined as the amount which will catalyze the transformation of 1 µmol substrate per minute. The v_{200} values were determined using 200 µM NAD(P)H on a 200 µL scale. For the determination of kinetic parameters, 10 mM maleimide was kept constant, while the concentration of NAD(P)H was varied between 20 µM and 1200 µM, whereby above 900 µM the assay volume was scaled to 150 µL. Kinetic parameters were estimated according to the Michaelis–Menten equation via nonlinear regression analysis (Sigma Plot 12.3, Systat Software, San Jose, CA).[39]

In order to determine the specific activities with (*R*)-carvone as substrate the assays were performed on a 10 mL scale using 500 µM NAD(P)H, 30 - 500 µg mL^{-1} purified enzyme, 10 mM (*R*)-carvone (added as an EtOH solution, < 5% final EtOH concentration) in sodium phosphate buffer (100 mM, pH 7.0). The reaction was initiated through the addition of cosubstrate, and data points were gathered for 5 min in 30 s intervals. Samples were immediately put on ice, in order to stop the reaction. Afterwards, the samples were extracted with 25% (v/v) EtOAc containing 7.2 mM (*R*)-limonene as internal standard. The more convenient sample storage on ice was preferred over direct extraction, since both strategies yielded in the same results.

Statistical information

Assays were performed in technical quintuplicates (n = 5) resulting in means μ_T and standard deviation σ_T. Additionally, between two (m = 2) and six (m = 6) biological replicates of these technical replicates were conducted, starting from individual single colonies. Combined biological means μ were calculated (Equation 1) using a relative weighting β_i for every technical mean $\mu_{T,i}$ (Equation 2).

$$\mu = \sum_{i=1}^{m} \mu_{T,i} \cdot \beta_i \qquad (1)$$

10.1002/adsc.201900073

$$\beta_i = \frac{\frac{1}{\sigma_i^2}}{\sum_{j=1}^{m} \frac{1}{{\sigma_{T,j}}^2}} \tag{2}$$

The corresponding standard deviation (σ) was calculated according to Equation 3.

$$\sigma = \sqrt{\sum_i (\mu_{T,i}^2 + {\sigma_{T,i}}^2) \cdot \beta_i - \mu^2} \tag{3}$$

Additional information

Supporting information is available for this paper, including further descriptions about applied materials and enzymes, cloning strategies, analytical procedures or homology modelling.

Correspondence and requests for materials should be addressed to K.C.

Acknowledgements

This work was supported by the 'BayBiotech' project association (www.baybiotech.de) financed by the Bavarian State Ministry of the Environment and Consumer Protection (grant number TLK01U-69036). The authors would like to thank Sophie v. Schönberg, Maurits Brinkman, Felix Schöpf, Fereshteh Sadeqi, David Auber, Konstantina Xypolia, Stephanie Grümbel or their help with the laboratory work as well as Sabine Wagner and Ingmar Polte for the fruitful discussions. The support of Christoph Mähler from the TUM Graduate School is acknowledged as well.

References

[1] T. Matsuda, R. Yamanaka, K. Nakamura, Tetrahedron: Asymmetry 2009, 20, 513–557.

[2] a) W. S. Knowles, *Adv. Synth. Catal.* **2003**, *345*, 3–13; b) R. Noyori, *Angew. Chem. Int. Ed.* **2002**, *41*, 2008–2022.

[3] a) K. Durchschein, M. Hall, K. Faber, *Green Chem.* **2013**, *15*, 1764; b) R. Stuermer, B. Hauer, M. Hall, K. Faber, *Curr. Opin. Chem. Biol.* **2007**, *11*, 203–213; c) H. S. Toogood, N. S. Scrutton, *Curr.*

Opin. Chem. Biol. **2014**, *19*, 107–115; d) A. Tosstorff, C. Kroner, D. J. Opperman, F. Hollmann, D. Holtmann, *Eng. Life Sci.* **2017**, *17*, 71–76.

[4] H. S. Toogood, J. M. Gardiner, N. S. Scrutton, *ChemCatChem* **2010**, *2*, 892–914.

[5] C. Breithaupt, J. Strassner, U. Breitinger, R. Huber, P. Macheroux, A. Schaller, T. Clausen, *Structure* **2001**, *9*, 419–429.

[6] R. M. Kohli, V. Massey, *J. Biol. Chem.* **1998**, *273*, 32763–32770.

[7] C. R. Pudney, S. Hay, N. S. Scrutton, *FEBS J.* **2009**, *276*, 4780–4789.

[8] A. Scholtissek, D. Tischler, A. Westphal, W. van Berkel, C. Paul, *Catalysts* **2017**, *7*, 130.

[9] E. D. Amato, J. D. Stewart, *Biotechnol. Adv.* **2015**, *33*, 624–631.

[10] C. K. Winkler, D. Clay, S. Davies, P. O'Neill, P. McDaid, S. Debarge, J. Steflik, M. Karmilowicz, J. W. Wong, K. Faber, *J. Org. Chem.* **2013**, *78*, 1525–1533.

[11] S. K. Padhi, D. J. Bougioukou, J. D. Stewart, *J. Am. Chem. Soc.* **2009**, *131*, 3271–3280.

[12] S. Reich, B. M. Nestl, B. Hauer, *ChemBioChem* **2016**, *17*, 561–565.

[13] J. T. Wu, L. H. Wu, J. A. Knight, *Clin. Chem.* **1986**, *32*, 314–319.

[14] C. You, R. Huang, X. Wei, Z. Zhu, Y.-H. P. Zhang, *Synthetic Syst. Biotechnol.* **2017**, *2*, 208–218.

[15] V. Uppada, S. Bhaduri, S. B. Noronha, *Curr. Sci.* **2014**, *106*, 946–957.

[16] A. M. Chánique, L. P. Parra, *Front. Microbiol.* **2018**, *9*, 1–14.

[17] J. K. B. Cahn, C. A. Werlang, A. Baumschlager, S. Brinkmann-Chen, S. L. Mayo, F. H. Arnold, *ACS Synth. Biol.* **2017**, *6*, 326–333.

[18] a) S. P. Miller, M. Lunzer, A. M. Dean, *Science* **2006**, *314*, 458–461; b) J. A. Rollin, T. K. Tam, Y.-H. P. Zhang, *Green Chem.* **2013**, *15*, 1708.

[19] J. K. B. Cahn, S. Brinkmann-Chen, T. Spatzal, J. A. Wiig, A. R. Buller, O. Einsle, Y. Hu, M. W. Ribbe, F. H. Arnold, *Biochem. J.* **2015**, *468*, 475–484.

[20] a) D. Cui, L. Zhang, S. Jiang, Z. Yao, B. Gao, J. Lin, Y. A. Yuan, D. Wei, *FEBS J.* **2015**, *282*, 2339–2351; b) S. Brinkmann-Chen, J. K. B. Cahn, F. H. Arnold, *Metab. Eng.* **2014**, *26*, 17–22.

[21] N. Borlinghaus, B. M. Nestl, *ChemCatChem* **2018**, *10*, 183–187.

[22] B. M. Nestl, B. Hauer, *ACS Catal.* **2014**, *4*, 3201–3211.

[23] R. Takase, B. Mikami, S. Kawai, K. Murata, W. Hashimoto, *J. Biol. Chem.* **2014**, *289*, 33198–33214.

[24] M. Nishiyama, J. J. Birktoft, T. Beppu, *J. Biol. Chem.* **1993**, *268*.

[25] R. Chen, A. Greer, A. M. Dean, *Proc. Natl. Acad. Sci.* **1996**, *93*, 12171–12176.

[26] T. Yaoi, K. Miyazaki, T. Oshima, Y. Komukai, M. Go, *J. Biochem.* **1996**, *119*, 1014–1018.

[27] a) A. Ochoa-Leyva, X. Soberón, F. Sánchez, M. Argüello, G. Montero-Morán, G. Saab-Rincón, *J. Mol. Biol.* **2009**, *387*, 949–964; b) A. Ochoa-Leyva, F. Barona-Gómez, G. Saab-Rincón, K. Verdel-Aranda, F. Sánchez, X. Soberón, *J. Mol. Biol.* **2011**, *411*, 143–157; c) M. V. Golynskiy, J. C. Haugner, B. Seelig, *ChemBioChem* **2013**, *14*, 1553–1563.

[28] H. Ma, T. M. Penning, *Proc. Natl. Acad. Sci.* **1999**, *96*, 11161–11166.

[29] E. Campbell, S. Chuang, S. Banta, *Protein Eng. Des. Sel.* **2013**, *26*, 181–186.

[30] Y. Fu, K. Castiglione, D. Weuster-Botz, *Biotechnol. Bioeng.* **2013**, *110*, 1293–1301.

[31] H.-B. Wang, X.-Q. Pei, Z.-L. Wu, *Appl. Microbiol. Biot.* **2014**, *98*, 705–715.

10.1002/adsc.201900073

[32] a) J. Tao, K. McGee, *Org. Process Res. Dev.* **2002**, *6*, 520–524; b) R. L. Hanson, S. L. Goldberg, D. B. Brzozowski, T. P. Tully, D. Cazzulino, W. L. Parker, O. K. Lyngberg, T. C. Vu, M. K. Wong, R. N. Patel, *Adv. Synth. Catal.* **2007**, *349*, 1369–1378; c) W. L. Parker, R. L. Hanson, S. L. Goldberg, T. P. Tully, A. Goswami, *Org. Process Res. Dev.* **2012**, *16*, 464–469.

[33] Y. Dong, K. J. McCullough, S. Wittlin, J. Chollet, J. L. Vennerstrom, *Bioorg. Med. Chem. Lett.* **2010**, *20*, 6359–6361.

[34] B. J. M. Jansen, J. A. Kreuger, A. d. Groot, *Tetrahedron* **1989**, *45*, 1447–1452.

[35] R. A. Sheldon, J. M. Woodley, *Chem. Rev.* **2018**, *118*, 801–838.

[36] I. Fichan, C. Larroche, C. B. Gros, *J. Chem. Eng. Data* **1999**, *44*, 56–62.

[37] a) R. A. Sheldon, P. C. Pereira, *Chem. Soc. Rev.* **2017**, *46*, 2678–2691; b) K. Castiglione, Y. Fu, I. Polte, S. Leupold, A. Meo, D. Weuster-Botz, *Biochem. Eng. J.* **2017**, *117*, 102–111.

[38] G. Fairbanks, T. L. Steck, D. F. H. Wallach, *Biochemistry* **1971**, *10*, 2606–2617.

[39] R. J. Ritchie, T. Prvan, *Biochem. Educ.* **1996**, *24*, 196–206.

10.1002/adsc.201900073

Graphical Abstract